# Electrophysiological Properties of Pyramidal Neurons in the Rat Prefrontal Cortex: An *In Vivo* Intracellular Recording Study

Eric Dégenètais, Anne-Marie Thierry, Jacques Glowinski and Yves Gioanni

INSERM U114, Chaire de Neuropharmacologie, Collège de France, 11 place Marcelin Berthelot, 75231 Paris Cedex 05, France

**In order to determine the electrophysiological properties of prefrontal cortex pyramidal neurons *in vivo*, intracellular recordings coupled with neurobiotin injection were performed in anesthetized rats. Three main classes of pyramidal cells were distinguished according to both their firing patterns in response to depolarizing current pulses and the characteristics of their action potentials: regular spiking (RS, $n = 71$); intrinsic (inactivating) bursting (IB, $n = 8$); and non-inactivating bursting (NIB, $n = 26$) cells. RS cells were further subdivided into slow-adapting and fast-adapting types, according to their firing frequency adaptation. IB and fast-adapting RS cells could exhibit different firing patterns depending on the intensity of the depolarizing current. In response to successive depolarizing pulses of a given intensity, NIB and some RS cells showed variations in their firing patterns, probably due to the impact of local synaptic activity. All the labeled neurons were pyramidal cells with an apical dendrite that formed a terminal tuft in layer I. As compared to RS cells, NIB cells had a smaller somatic size and their apical dendritic tuft was less extensive, while IB cells presented a larger somatic size, thicker dendrites and a wider extent of their basal and apical dendritic arborization. In conclusion, we found in the rat prefrontal cortex, *in vivo*, different electrophysiological classes of pyramidal cells whose output firing patterns depend on interactions between their intrinsic properties and the ongoing synaptic activity.**

## Introduction

The prefrontal cortex (PFC) is involved in higher cognitive functions such as working memory, temporal ordering events, organization and planning of responses (Goldman-Rakic, 1995a,b; Seamans *et al*., 1995; Floresco *et al*., 1997; Fuster, 1997). Among various mammalian species, the PFC is defined as the cortical region that receives its main thalamic inputs from the mediodorsal nucleus of the thalamus (Rose and Woolsey, 1948; Groenewegen, 1988). The PFC is connected with associative cortical areas and with subcortical structures of the extrapyramidal and limbic systems (Uylings and Van Eden, 1990) and is innervated by the ascending monoaminergic (noradrenergic, dopaminergic, serotonergic) and cholinergic systems.

Pyramidal cells, which represent the major neuronal population of the cerebral cortex, are the output neurons that integrate and transfer information from extra-cortical inputs and local circuits to distant cortical areas and sub-cortical structures. Several electrophysiological classes of pyramidal neurons have been characterized, mainly on the basis of their response to application of prolonged intracellular current pulses as well as the shape of their action potentials (Connors and Gutnick, 1990). These electrophysiological properties have been mostly analysed from *in vitro* studies performed on the rat and guinea pig cerebral cortex. Two main classes of pyramidal neurons have been described: the regular spiking (RS) and the intrinsic bursting (IB) cells (Connors *et al*., 1982; Stafstrom *et al*., 1984; McCormick *et al*., 1985; Chagnac-Amitai *et al*., 1990; Mason and Larkman, 1990; Van Brederode and Snyder, 1992; Kang and Kayano, 1994). The *in vivo* electrophysiological characteristics of pyramidal cells have only been described in a few reports. In addition to RS and IB cells, two additional classes of pyramidal cells were revealed in these *in vivo* studies: the fast-adapting RS cells and the non-inactivating bursting cells (NIB), which were found in the cat associative and motor cortex, respectively (Baranyi *et al*., 1993a; Nuñez *et al*., 1993).

The electrophysiological characteristics of PFC pyramidal cells have been analysed in a few *in vitro* studies that have also revealed the presence of RS and IB pyramidal cells (de la Peña and Geijo-Barrientos, 1996; Yang *et al*., 1996). However, the *in vivo* electrophysiological properties of PFC pyramidal cells still remain to be determined. Therefore, the present study was undertaken to investigate the basic electrophysiological features of pyramidal cells of the rat PFC, using both *in vivo* intracellular recording and staining. No attempt was made to investigate local inhibitory interneurons.

## Materials and Methods

### *Animal Surgery*

Experiments were conducted in 77 adult male Sprague–Dawley rats weighing 275–300 g. Animals were initially anesthetized with sodium pentobarbital (66 mg/kg, i.p.) and mounted in a stereotaxic apparatus. Anesthesia was maintained throughout the experiments by additional doses of sodium pentobarbital (22 mg, i.p) administrated hourly. The level of anesthesia was assessed by testing the limb withdrawal reflex, additional doses of anesthetic being injected if needed to ensure areflexia. Wounds and pressure points were repeatedly infiltrated with lidocaine (xylocaine 2%). Stability of recordings was ensured by cisternal drainage. Body temperature was maintained at 36.5°C with a homeothermic blanket.

### *Electrophysiological Procedures*

Glass microelectrodes (50–80 MΩ resistance) were filled with 1 M K-acetate containing 1% neurobiotin to achieve labeling of recorded neurons. Intracellular recordings were performed in the prelimbic/medial orbital area of the PFC, using the following stereotaxic coordinates: anterior, +3–4 mm from bregma; lateral, 0.4–1 mm from the midline; and depth, 2–4 mm from the cortical surface (Paxinos and Watson, 1997). All recordings were obtained using an Axoclamp-2B amplifier (Axon Instruments, Foster City, CA) operated in the bridge mode. Impalements of neurons were considered acceptable when the membrane potential was at least –60 mV and the spike amplitude >50 mV. Signals were stored on digital audiotape (DTR-1800, Biologic, France) and subsequently digitized using a CED 1401 interface (sampling frequency, 16 kHz). Data were analysed off-line using Spike2 software (Cambridge Electronic Design, Cambridge, UK).

Classification of the different PFC cell types was based on their responses to intracellular application of prolonged (400 ms) depolarizing current pulses (Connors *et al*., 1982). Spike threshold, defined as the membrane potential corresponding to the slope break point, was expressed as the mean membrane potential at which spontaneous action potentials were triggered. In cells that did not exhibit spontaneous firing,

**Table 1**
Electrical properties of different neurons classes of the prefrontal cortex

| Electrophysiological classes (*n*) | $V_m$ (mV) | $R_N$ (MΩ) | Spike amplitude (mV) | Spike duration (ms) | Spike threshold (mV) | Rheobase (nA) |
|---|---|---|---|---|---|---|
| Slow-adapting RS (71) | –68.7 ± 5.3 | 34.6 ± 10.6 | 61.0 ± 7.0 | 1.80 ± 0.42 | –50.8 ± 5.8 | 0.30 ± 0.15 |
| Fast-adapting RS (10) | –70.5 ± 2.6 | 33.8 ± 15.2 | 54.9 ± 4.6 | 1.92 ± 0.24 | –48.5 ± 3.9 | 0.42 ± 0.20* |
| IB (8) | –68.5 ± 2.8 | 23.5 ± 6.9** | 66.6 ± 8.3 | 2.10 ± 0.50 | –55.5 ± 5.4 | 0.25 ± 0.13 |
| NIB (26) | –68.4 ± 5.0 | 42.3 ± 12.3** | 60.1 ± 6.8 | 1.91 ± 0.53 | –51.7 ± 5.3 | 0.23 ± 0.16 |

All data are expressed as mean ± SD. Data of the different classes of cells are compared with those of slow- adapting RS cells; *t*-test, two-tailed P values. *$P < 0.05$; **$P < 0.005$.

the threshold was determined for the first spike evoked by a depolarizing intracellular current pulse. Spike duration was measured as the time needed by the membrane potential to rise from the voltage threshold and return to this potential. The rheobase was measured as the lowest current intensity leading to spike discharge from resting potential (pulses of 400 ms duration). The amplitude of the action potentials was measured as the difference between the threshold potential and the peak potential of the spike waveform. To assess the input resistance ($R_N$) of neurons, we measured the average voltage response ($n$ = 10) to the injection of hyperpolarizing current pulses of weak intensity (100 ms duration, 0.3 nA, 0.3 Hz) through the recording electrode. Current–voltage (*I–V*) relationships were established by injecting square-wave current pulses (100 ms duration) with increasing intensity (from –1.2 nA up to supra-threshold positive current by 0.2 nA steps). Voltage responses were measured at the end of pulses and averaged from 5 to 10 responses. The study of the membrane voltage response in the depolarizing range was in most cases limited by the triggering of action potentials. The resting membrane potential ($V_m$) was calculated by subtraction of the tip potential occurring when the microelectrode was withdrawn from the neuron. The spontaneous firing frequency was calculated from 1 min periods.

Student's unpaired *t*-test was used to compare electrophysiological parameters across the different populations of PFC pyramidal neurons.

### *Histological Methods*

Following the electrophysiological characterization of a neuron, an intracellular injection of neurobiotin (Vector) was performed by passing a depolarizing current pulse (100 ms, 0.3–0.6 nA, 1 Hz) over 5–15 min. Then, the rat was deeply anesthetized with sodium pentobarbital (200 mg/kg, i.p.) and perfused intra-cardially with a 0.9% saline solution containing 1% sodium nitrite, followed by fixative solution (4% paraformaldehyde/0.1% glutaraldehyde in 0.1 M sodium phosphate buffer). The brain was removed and, following 4 h post-fixation in a 4% paraformalde-hyde phosphate-buffered solution, stored for 48 h in 20% phosphate-buffered sucrose. Frontal sections (50 μm) were cut on a freezing microtome and collected in 0.1 M potassium phosphate-buffered saline (pH 7.4). After three washes in 0.1 M sodium phosphate buffer (pH 7.4), slices were incubated for 12 h in 1% avidin–biotin complex (ABC Kit Standard, Vector Laboratories) in the presence of 0.5% Triton X-100. After three rinses in phosphate buffer, slices were reacted in diaminobenzidine (1%) and cobalt chloride (1%)/nickel ammonium sulfate (1%)/$H_2O_2$ (0.01%) solution. The position of the stimulating electrode was marked by an electrical deposit of iron (6 μA positive current, 20 s) and observed on histological sections following a ferri-ferrocyanide reaction.

### *Anatomical Analysis*

Labeled neurons and boundaries of PFC layers were traced and reconstructed from successive serial sections. To achieve 3D reconstructions, cell bodies, dendritic arborizations and layer boundaries were drawn under 10–40× objectives of a light microscope (Olympus) and plotted in 3D using Neurolucida video computer software (Microbrightfield Inc.). Several morphological parameters of the labeled neurons were measured: the area of the soma section at its highest value and the maximal dimension of the basilar dendritic field and the apical dendritic tuft. The dorso-ventral extension of the dendritic field was determined by measuring the extremities of the dendritic field along an axis parallel to the medial cortical surface. The rostro-caudal extension of the dendritic field was determined by measuring the length of the dendritic field along an axis orthogonal to the section plane. Student's unpaired *t*-test was used to compare somatic size and the extension of the dendritic fields.

## Results

Data were obtained from 115 neurons located in layers II–VI of the medial PFC. Three main classes of pyramidal cells were distinguished on the basis of their evoked firing pattern in response to intracellular prolonged depolarizing pulses. Cells were classified as regular spiking (RS), non-inactivating bursting (NIB) and intrinsic (inactivating) bursting (IB) cells.

### *RS Cells*

Eighty-one of the recorded cells (70%) were classified as RS cells. These cells were characterized by a sustained discharge in response to depolarizing current pulses having an intensity >0.5 nA. RS cells were further classified as slow-adapting and fast-adapting, according to the spike frequency adaptation during their evoked discharge.

#### *Slow-adapting RS cells*

Seventy-one of the RS cells (87%) were classified as slow-adapting RS cells. These cells presented a sustained firing for depolarizing pulses of intensity >0.50 ± 0.16 nA, while they discharged only a few spikes at lower intensities. The mean rheobase of these cells was 0.30 ± 0.15 nA (Table 1). The sustained discharge consisted of two or three initial action potentials (doublet, triplet) with inter-spike intervals (ISIs) shorter than those of following action potentials. These cells had a mean resting membrane potential ($V_m$) of –68.7 ± 5.3 mV, a mean input resistance ($R_N$) of 34.6 ± 10.6 MΩ and a mean firing threshold of –50.8 ± 5.8 mV. Action potentials had a mean amplitude of 61.0 ± 7.0 mV and a mean duration of 1.80 ± 0. 42 ms (Table 1). Two groups of slow-adapting RS cells were distinguished on the basis of their frequency adaptation and spike characteristics.

In the first group of slow-adapting RS cells, named group I, ($n$ = 47) the discharge induced by a depolarizing current pulse showed a light or no adaptation in frequency after the initial doublet or triplet of spikes (Fig. 1*A*,*B*,*C*). Spikes exhibited a fast after-hyperpolarization (fAHP) of 2–5.3 mV amplitude and 0.8–1.5 ms duration. During the initial doublet or triplet, spike threshold slightly increased, no slow after-hyperpolarization (sAHP) was observed and a depolarizing after-potential (DAP) occurred in 60% of the cells after the initial spike (Fig. 1*A*). During the steady state discharge, the firing threshold remained constant, the spikes were followed by a prominent sAHP (amplitude, 4.4–9 mV; duration, 33–82 ms) that showed no obvious variation and no DAP was observed (Fig. 1*A*,*B*). Finally, at the cessation of the depolarizing pulse, an undershoot of the membrane potential was generally observed (Fig. 1*A*, upper trace).

Only 45% of group I slow-adapting RS cells ($n$ = 21) presented a spontaneous firing (mean frequency: 0.90 ± 1.23 Hz) which mainly consisted in single action potentials. In five cells, doublets were also observed. Spontaneous spikes were followed in all cases by an fAHP and, in some cases, by a DAP, but sAHPs were not detectable (Fig. 1*D*).

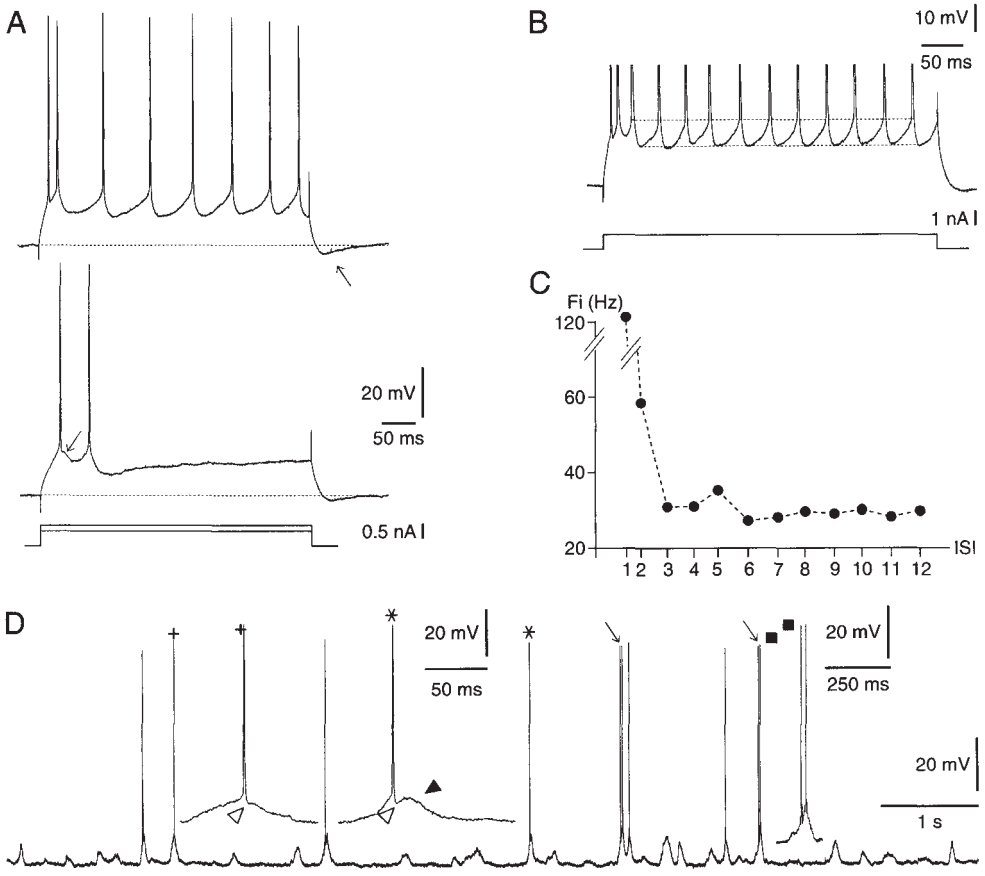


**Figure 1.** Electrophysiological characteristics of group I slow-adapting RS cells. (*A*) A depolarizing current pulse of 0.7 nA (upper trace) evoked an initial doublet of action potentials followed by a regular discharge. Note the undershoot at the cessation of the hyperpolarizing pulse (arrow). A lower intensity current pulse (0.5 nA, lower trace) evoked only a few spikes. Note that only the first spike was followed by a DAP (arrow). Resting membrane potential: –72 mV (dashed lines). (*B*) Magnified view of the discharge evoked by a current of 1 nA in another cell (spikes are truncated). Note that the spike threshold (upper dashed line) remained quite constant throughout the regular discharge phase. Resting membrane potential: –70 mV. (*C*) Plot of the instantaneous spike frequency against ISIs during the response shown in (*B*). After the strong adaptation during the initial triplet of spikes, the frequency remained quite constant. (*D*) Spontaneous firing of another cell, consisting in single spikes and doublets (doublets are marked by an arrow). Insets: magnified views of single spikes (identified by the cross and the star) and of a doublet (filled square). All the spikes showed fAHPs (open arrowhead) and some spikes presented a DAP (filled arrowhead).

In the second group of slow-adapting RS cells ($n$ = 24), named group II, the sustained discharge evoked by depolarizing current pulses >0.50 ± 0.15 nA showed a progressive adaptation in frequency (Fig. 2*A*,*B*,*C*). In all cases, spikes presented fAHPs (amplitude, 4–9 mV; duration, 1.2–2.6 ms) more prominent than those of group I cells. The fAHP observed in group II cells was not followed by a DAP. In contrast to group I slow-adapting RS cells, following the initial doublet or triplet, the firing voltage threshold progressively increased (Fig. 2*B*). The mean increase of the firing threshold, measured between the first spike after the initial doublet and the last spike of the evoked discharge, was 4.3 ± 1.7 mV. During this discharge, spikes were followed by a biphasic sAHP (amplitude, 4.8–10 mV; duration, 22–64 ms) and the progressive increase of successive ISIs was concomitant with a progressive lengthening of the second phase of the sAHPs (Fig. 2*A*,*B*). At the cessation of depolarizing pulses, no obvious undershoot was observed (Fig. 2*A*).

Spontaneous firing was observed in 13 group II cells (55%) and consisted in isolated spikes. The mean frequency (0.62 ± 0.75 Hz) was not significantly different from that of group I cells. Spontaneous action potentials were followed by a prominent fAHP, no DAPs were observed and sAHPs were not detectable (Fig. 2*D*).

Some slow-adapting RS cells (six cells in group I and seven in group II) showed variable patterns of discharge in response to application of depolarizing current pulses of similar intensity. As shown in Figure 3, the discharge patterns consisted of either a sustained discharge or a discharge interrupted by hyperpolarization periods or an initial train of spikes followed by an irregular discharge. The interruption of the firing by hyperpolarizing potentials strongly suggests that these neurons received synaptic inputs sufficient to alter their sustained discharge.

*Fast-adapting RS Cells*

In response to application of relatively high intensity depolarizing current pulses (>0.6 nA), 10 neurons presented an initial train of spikes (3–11 spikes) followed by a depolarizing plateau (Figs 4 and 5*A2*). According to Nuñez *et al.* (Nuñez *et al.*, 1993), who have described a similar firing pattern in the cat motor cortex, these cells were named 'fast-adapting RS cells'.

The duration of the train of spikes was slightly lengthened by increasing the depolarizing current intensity and its maximal mean duration was 83 ± 21 ms. Within the train, the ISIs progressively increased during the discharge and the spike amplitude showed slight variations (Fig. 4*A2*). When high intensity currents (mean threshold intensity: 1.0 ± 0.4 nA) were applied, the train was followed by a slow depolarization (Figs 4*A2* and 5*A2*, arrowheads).

In five of these cells, depolarizing pulses of moderate current intensities (0.2–0.5 nA) elicited a sustained discharge (Fig. 5*A1*),

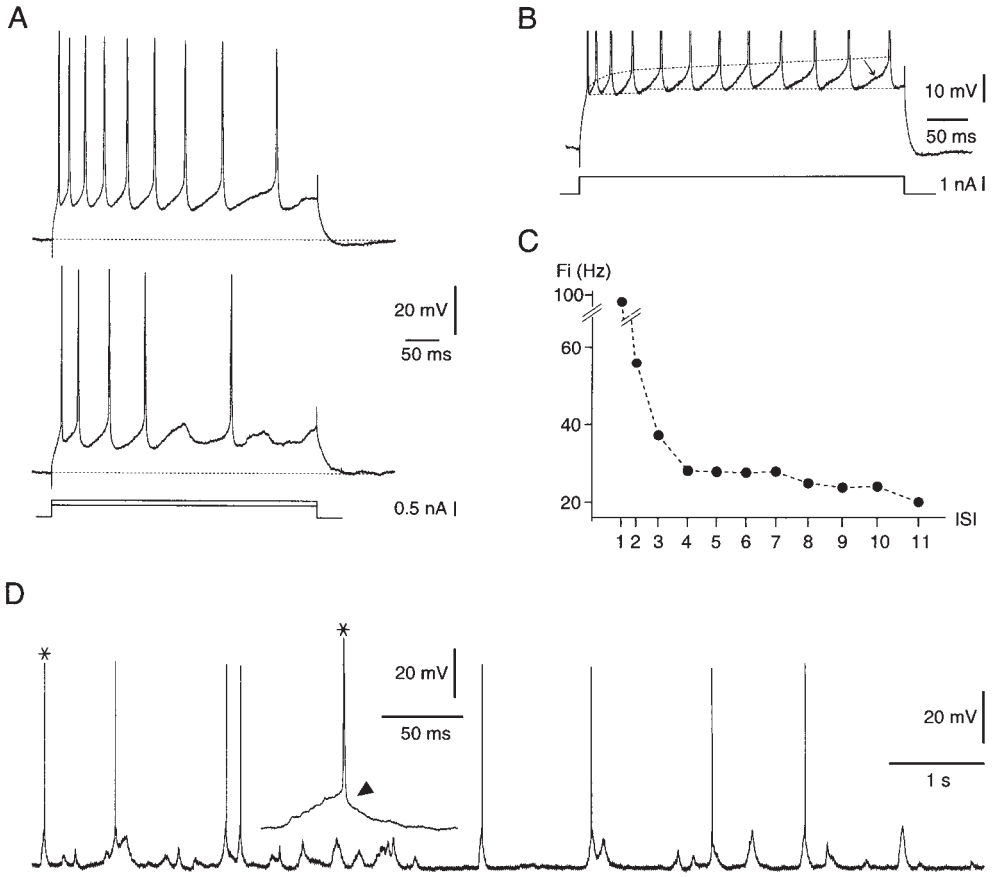


**Figure 2.** Electrophysiological characteristics of group II slow-adapting RS cells. (*A*) A depolarizing current pulse of 0.7 nA (upper trace) induced a tonic discharge with frequency adaptation. A lower intensity current pulse (0.5 nA) evoked only a few spikes (lower trace). Resting membrane potential: –72 mV (dashed lines). (*B*) Magnified view of the discharge evoked by a current of 1.2 nA in another cell (spikes are truncated). Note the progressive increase of the spike threshold during the tonic discharge (upper dashed line), and the increase in duration of the second phase of the successive AHPs (arrow). Resting membrane potential: –68 mV. (*C*) Plot of the instantaneous spike frequency against ISIs during the response shown in (*B*). After the strong adaptation during the initial discharge, the spike frequency displayed a progressive decrease. (D) The spontaneous firing consisted of single spikes [same cell as in (*A*)]. Inset: magnified view of the spike marked by a star. Note the pronounced fAHP (filled arrowhead).

but successive identical current pulses evoked variable patterns of discharge that consisted either in a sustained firing or in an irregular discharge (Fig. 5*A1*, lower trace). For depolarizing currents of 0.5–0.6 nA, these cells exhibited a transitional pattern of discharge, consisting in an initial train followed by a few isolated spikes (Fig. 5*A2*, lower trace). Finally, for higher current intensities (>0.6 nA), the initial train was followed by a depolarizing plateau (Fig. 5*A2*, upper trace).

Action potentials of fast-adapting RS cells were followed by a prominent fAHP (amplitude, 3.6–9.2 mV; duration, 1.2–2.4 ms), whereas sAHPs (amplitude, 2.9–13.4 mV; duration, 11–55 ms) were only observed after isolated spikes (evoked by low intensity current pulses; Fig. 5*A1*).

Fast-adapting RS cells never presented spontaneous firing, even though fast oscillations of their membrane potentials were observed (Figs 4*B* and 5*B*).

### *IB Cells*

Eight neurons that exhibited bursts of three to five spikes of decreasing amplitude and increasing duration, riding upon a slow depolarizing envelope, were classified as IB cells according to the definition of Connors *et al.* (Connors *et al.*, 1982). Because, within a burst the successive spikes inactivated, this class of cells has also been denominated 'inactivating-bursting' (Baranyi *et al.*, 1993a). The mean frequency of spikes within a burst was 77 ± 21 Hz. As shown in Figure 6*A* (lower trace), depolarizing current pulses of low intensities (0.2–0.5 nA) could trigger bursts in addition to isolated spikes. The all-or-none character of bursts is illustrated in Figure 6*B*, which shows that a short duration depolarizing current pulse induced a burst that outlasted the duration of the pulse. For higher current intensities, a sustained discharge was observed during which bursts occasionally occurred (Fig. 6*A*, middle trace, arrow). However, for current intensities of 0.8–1 nA, bursts were no longer observed and the discharge of IB cells was similar to that of RS cells (Fig. 6*A*, upper trace). A small undershoot of the membrane potential was observed at the end of the depolarizing pulses. The rheobase and the spiking threshold of IB cells were similar to those of RS cells (Table 1). At the cessation of hyperpolarizing pulses, a depolarizing membrane potential rebound was observed which could give rise to either an isolated spike or a burst (Fig. 6*C*).

Basic membrane properties of IB cells were similar to those of RS cells, except for the $R_N$, which was significantly lower (Table 1). Single spikes were followed by a DAP and in some cases by an fAHP. An sAHP (amplitude, 1–5.6 mV; duration, 21–76 ms) occurred following both single spikes and bursts (Fig. 6*A*).

All IB cells showed spontaneous firing, the frequency of which was significantly higher than that of spontaneously active

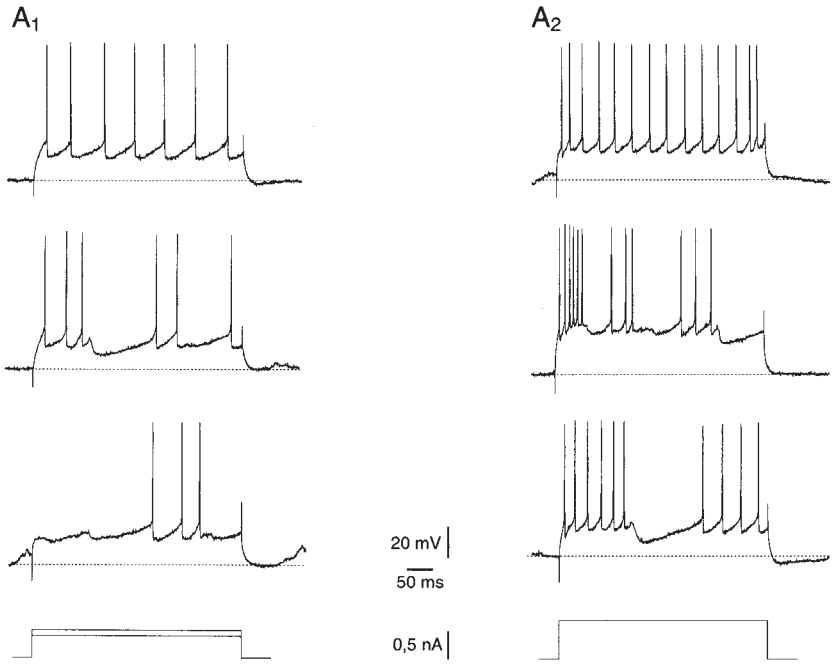


**Figure 3.** Typical example of a slow-adapting RS cell with variable firing patterns. (*A1*) A low intensity depolarizing current pulse (0.4 nA, lower trace) triggered only a few spikes. A higher current intensity (0.5 nA) depolarizing pulse evoked either an irregular (middle trace) or a regular (upper trace) discharge. (*A2*) Increasing the depolarizing current intensity (0.7 nA) resulted in an increase of the firing frequency. From top to bottom: note that the discharge pattern was variable for similar successive pulses. Resting membrane potential: –63 mV (dashed lines).

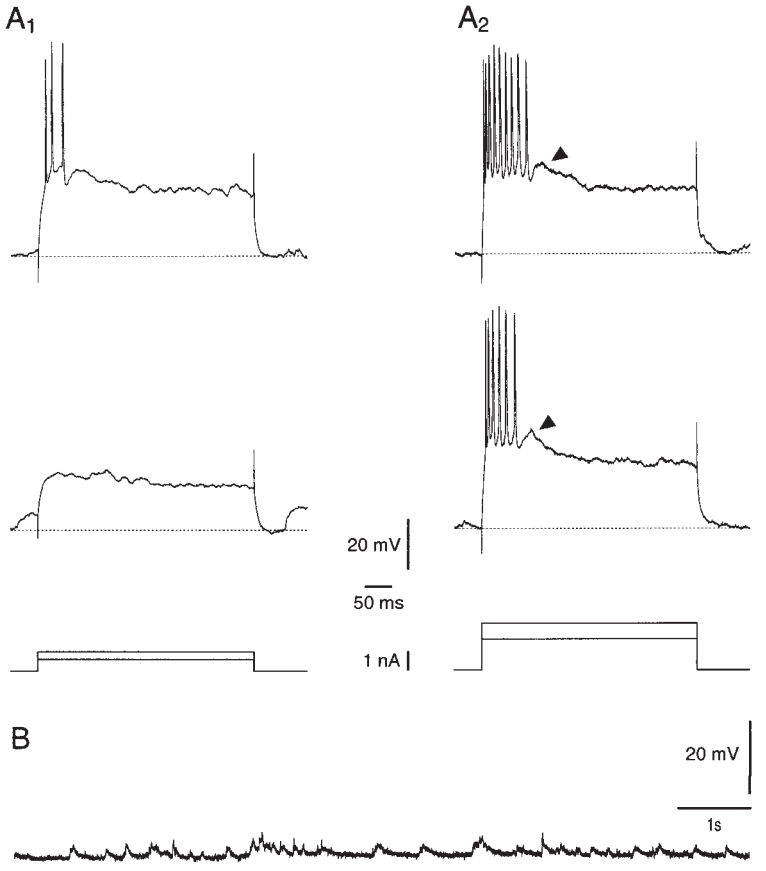


**Figure 4.** Electrophysiological characteristics of fast-adapting RS cells. (*A1*) Responses to a sub-threshold (0.6 nA, lower trace) and to a near threshold (0.8 nA, upper trace) current depolarizing pulse. (*A2*) Responses of the same cell to higher intensities current pulses (1.6 nA, bottom trace; 2.4 nA, upper trace). Suprathreshold current pulses always evoked an initial spike train of limited duration. Note the slow depolarization (arrowheads) that followed the spike train. (*B*) The spontaneous activity of the cell was characterized by a lack of spontaneous firing. Resting membrane potential: –76 mV (dashed lines).

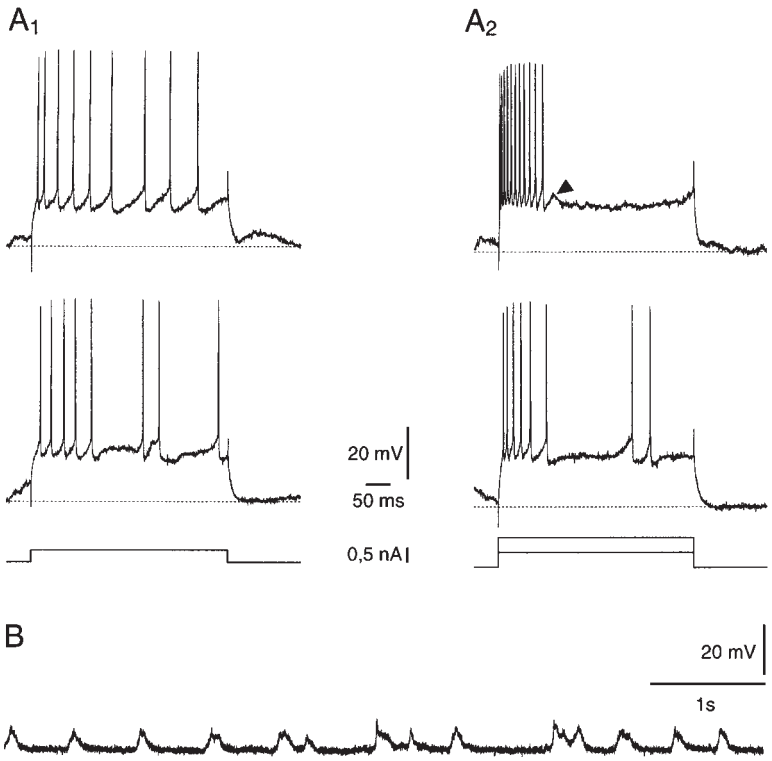


**Figure 5.** Example of a fast-adapting RS cell with variable firing patterns. (*A1*) Successive low intensity (0.4 nA) depolarizing current pulses evoked either an irregular (lower trace) or a regular (upper trace) discharge. (*A2*) A high current pulse intensity (1 nA, upper trace) elicited only an initial train of spikes. Note the slow membrane depolarization at the end of the discharge (arrowhead). For an intermediate current pulse intensity (0.5 nA, lower trace) the cell discharged an initial spike train followed by a few spikes. (*B*) The spontaneous activity of the cell was characterized by a lack of spontaneous firing. Resting membrane potential: –67 mV (dashed lines).

RS cells (3.1 ± 2.6 Hz, $P < 0.005$). In these cells, frequent spontaneous EPSPs occurred and produced either isolated action potentials or bursts similar to those evoked by a depolarizing pulse (Fig. 6*D*,*E*). Spontaneous action potentials were followed by a DAP; an fAHP occurred in some cases following single spikes (Fig. 6*D*, right) and sAHPs were not observed (Fig. 6*E*).

### *NIB Cells*

Twenty-six cells presented, in response to depolarizing current pulses, all-or-none bursts of 3–8 action potentials that did not inactivate (Fig. 7) and have been denominated 'non-inactivating bursting cells' according to Baranyi *et al.* (Baranyi *et al.*, 1993a). Within a burst, the duration of successive spikes increased, due to a slowing of the repolarization phase (Fig. 7*B*) and the mean durations of the first and last spikes were 1.9 ± 0.4 and 4.3 ± 1.4 ms ($n$ = 19), respectively. In addition, the firing threshold progressively increased from the first to the last spike of a burst (mean increase: 3.6 ± 2.2 mV, $n$ = 18). The mean firing frequency within the burst (92 ± 39 Hz, $n$ = 20) was not significantly different from that of IB cells. In contrast to IB cells, the probability of eliciting bursts in NIB cells increased with the intensity of the depolarizing current.

As IB cells, NIB cells exhibited variable patterns of discharge in response to successive depolarizing current pulses of a given intensity. Indeed, for near-threshold current pulses of similar intensities, the discharge consisted either in a few isolated spikes or doublets or, less frequently, in an initial burst of three spikes (Fig. 7*A1*). Supra-threshold depolarizing pulses of a given intensity resulted in either a sustained regular firing similar to that of RS cells (Fig. 7*A2*, upper trace), or an irregular discharge (Fig. 7*A2*, middle trace), or an initial burst followed by an irregular discharge (Fig. 7*A2*, lower trace). At the break of the depolarizing pulses, the membrane potential exhibited no obvious or only a slight undershoot.

Basic electrical membrane properties of NIB cells were similar to those of RS cells, except for $R_N$, which was significantly higher (Table 1). A well-developed fAHP (amplitude, 2.9–8.7 mV; duration, 0.7–1.4 ms) was observed after the first spike of doublets and bursts (Fig. 7*B*), as well as after the single action potentials elicited by a depolarizing current pulse (Fig. 7*A2*), whereas sAHPs (amplitude, 2.2–10 mV; duration, 10–80 ms) were mostly seen after isolated spikes. DAPs occurred within the doublets and bursts, but were rarely observed after isolated spikes (Fig. 7*B*).

All NIB cells presented a spontaneous firing consisting of isolated spikes, frequent doublets and bursts of three to six spikes (Fig. 7*B*). The mean frequency of spontaneous discharge of these cells was similar to that of IB cells, but significantly higher than that of RS cells (2.8 ± 3.2 Hz, $P < 0.05$). The characteristics of action potentials were similar in spontaneous and evoked doublets or bursts. Spontaneous isolated action potentials were followed by an fAHP and in all cases by a DAP.

### *I–V Relationships*

The *I–V* curves were established for 41 cells. They show that the majority of these cells (85%) presented an inward rectification for potentials 5–20 mV more polarized than the resting membrane potential (Fig. 8*A*, left). In remaining cells, *I–V* curves were linear (Fig. 8*A*, right). No correlation was found between the electrophysiological classes of cells described above and the characteristics of *I–V* curves. Cells exhibiting an inward rectification were observed in all electrophysiological classes and cells with a linear *I–V* curve belonged to RS and NIB classes.

Application of an intracellular hyperpolarizing pulse induced

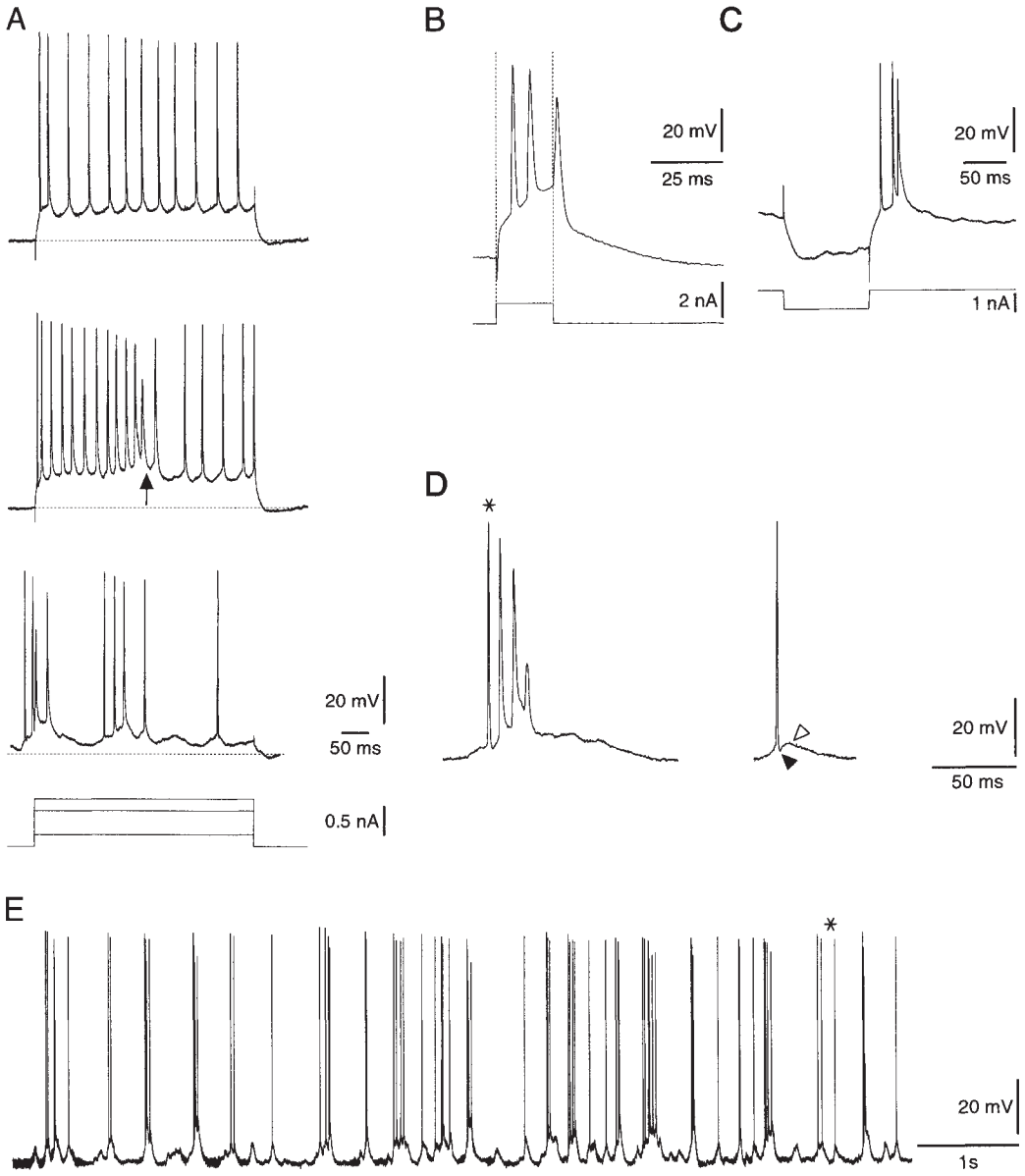


**Figure 6.** Electrophysiological characteristics of IB cells. (*A*) Near threshold depolarizing current pulses (0.2 nA, lower trace) triggered bursts and single action potentials. Increasing current intensity (0.6 nA, middle trace) elicited a sustained discharge during which bursts could still occur (arrow). For a higher current intensity (0.8 nA, upper trace), the cell displayed an RS-like pattern and no burst was observed. (*B*) A short-duration depolarizing current pulse (duration, 20 ms; intensity, 1.2 nA) could trigger a burst in an all-or-none fashion, even for a pulse duration shorter than that of the burst. (*C*) A rebound response that triggered a burst was observed at the cessation of a hyperpolarizing current pulse (duration, 100 ms; intensity, –1.0 nA). (*D*) Magnified view of the spontaneous burst marked by star in (*E*) (left) and of a spontaneous single spike (right). Note the strong inactivation of the spikes along the burst. The single spikes were followed by an fAHP (filled arrowhead) and by a DAP (open arrowhead). (*E*) Spontaneous activity consisting in single spikes, doublets and bursts. The star indicates the burst magnified in (*E*). Resting membrane potential: –65 mV (horizontal dashed lines).

depolarizing sag of the membrane potential only in group I slow-adapting RS cells (Fig. 8*B*). At the cessation of the hyperpolarizing pulse, a depolarizing rebound occurred in all classes of cells, with the exception of group II slow-adapting RS and fast-adapting RS cells (Fig. 8*B*). The rebound could trigger single spikes or a burst in IB cells and one or two spikes in group I slow-adapting RS and NIB cells.

### *Cell Morphology*

All recorded cells injected with neurobiotin ($n$ = 41) had morphological features of pyramidal neurons, namely the presence of apical and basal dendrites with numerous spines.

#### *RS Cells*

Among the 30 labeled RS cells, 25 cells had their soma located in deep layers (V and VI) and five cells in superficial layers II and III (Table 2). The soma of RS cells of deep layers had an average area of 307 ± 61 $\mu m^2$ and was surrounded by a well-developed basal dendritic field, the maximal extent along the dorso-ventral and rostro-caudal axis of which were of 202 ± 60 and 177 ± 66 μm, respectively. The apical dendrite gave off a few branches in layers V and II/III, before reaching up to layer I, where it divided into an apical tuft (Figs 9*A* and 10). The maximal extent of the apical arbor and of the basal dendritic field were not significantly different (234 ± 100 μm dorso-ventral, range, 120–400 μm and 157 ± 113 μm rostro-caudal, range, 100–400 μm, respectively).

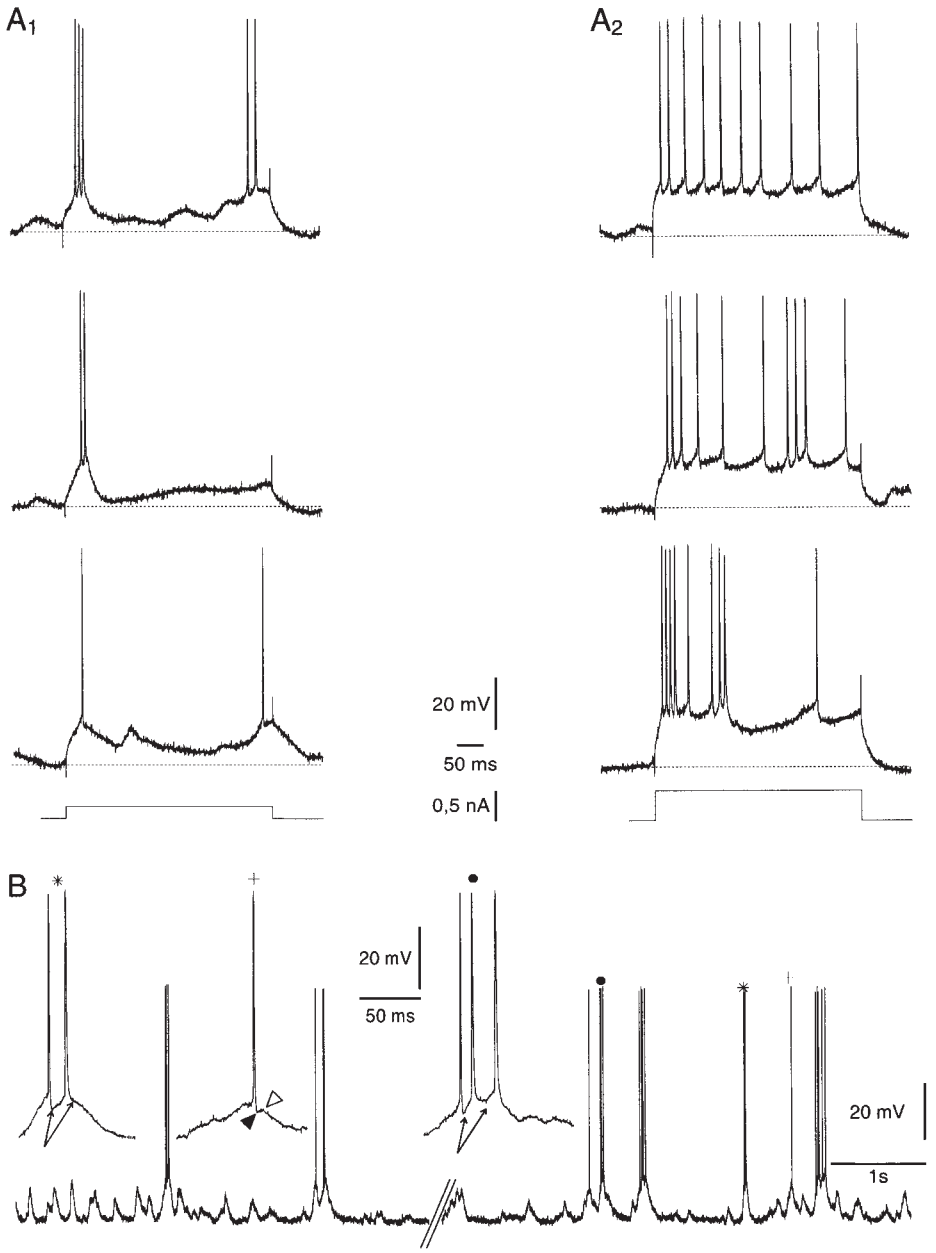


**Figure 7.** Electrophysiological characteristics of NIB cells. (*A1*) A near threshold depolarizing pulse (intensity, 0.2 nA) evoked either a few spikes or a doublet or a burst. (*A2*) In the same cell, a higher intensity current pulse (0.5 nA) evoked either a regular discharge (upper trace) or an irregular firing with single spikes (middle trace) or bursts (lower trace). (*B*) The spontaneous activity consisted in single spikes, doublets and non-inactivating bursts (an other cell). Symbols on the trace show the spike, doublet and burst magnified in the insets. Middle inset: single spike followed by an fAHP (filled arrowhead) and a DAP (open arrowhead). Left inset: doublet of spikes. Right inset: a three-spike non-inactivating burst. Note that in doublets and bursts, an fAHP was present only after the first spike (arrows). Resting membrane potentials: –72 mV (*A*, dashed lines) and –70 mV (*B*).

The soma of superficial layers RS cells had an average area of 239 ± 48 μm$^2$ and was surrounded by a well-developed basal dendritic arbor within layer II/III that extended in a few cases into layer V. In layer I, the apical dendrite formed a terminal arbor (Figs 9*C* and 10). The maximal extent of the basal dendritic field (dorso-ventral, 210 ± 86 μm and rostro-caudal, 200 ± 70 μm) and of the apical dendritic arbor (dorso-ventral, 270 ± 144 μm and rostro-caudal, 157 ± 53 μm) was comparable to that of the deep layers RS cells.

*NIB Cells*

Eight NIB cells were labeled. For seven cells, the soma was located in the deep layers (layers V and VI; Table 2). The soma of these cells (maximal average area 264 ± 46 μm$^2$) appeared smaller than that of deep layers RS cells (Figs 9*B* and 10), but the difference did not reach statistical significance. The maximal extent of their basal dendrites (dorso-ventrally, 212 ± 85 μm, range, 150–300 μm and rostro-caudally, 180 ± 27 μm, range, 150–200 μm) was similar to that of RS cells located in layers V and VI. The apical dendrites of these cells, which appeared thinner than those of deep layers RS cells, gave off a few branches in layer V and II/III and then reached layer I where they divided into an apical tuft (dorso-ventral extent, 147 ± 52 μm, range, 100–320 μm and rostro-caudal extent, 137 ± 62 μm, range, 150–400 μm).

The labeled NIB cell with a soma (188 μm$^2$) located in

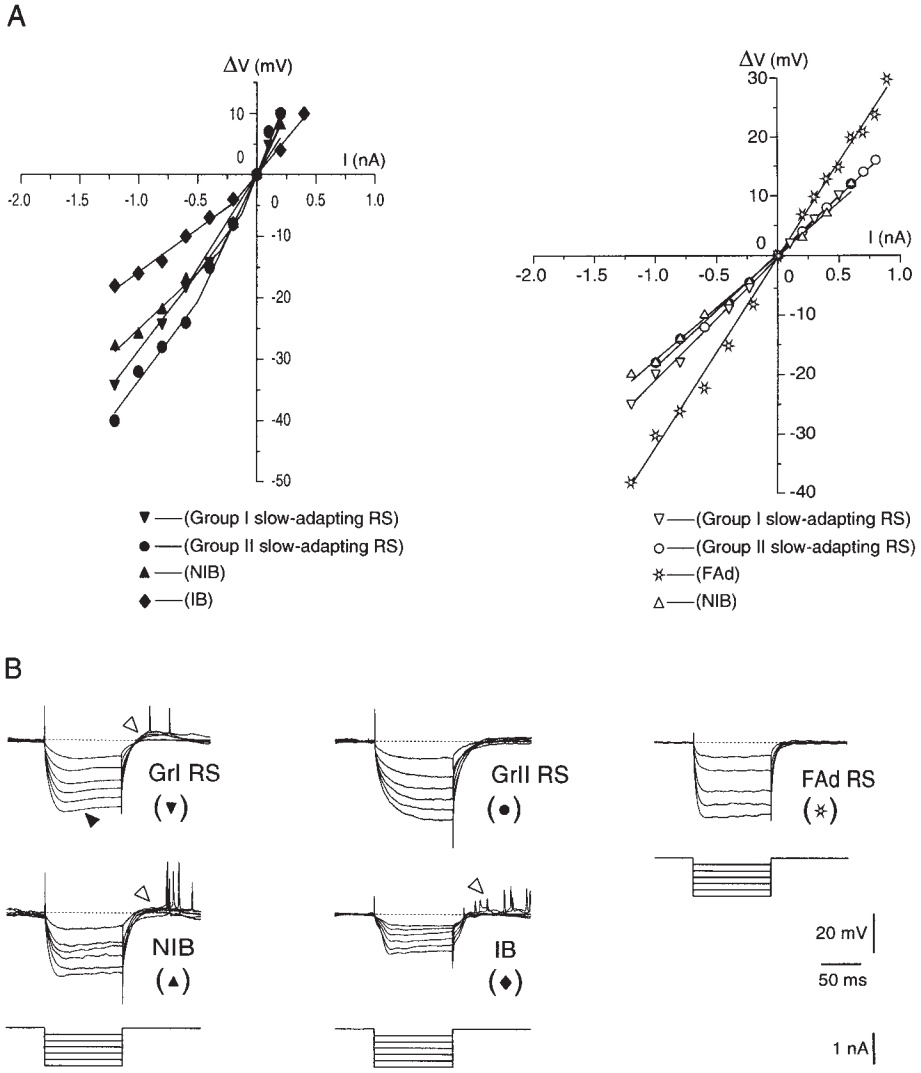


**Figure 8.** Typical current–voltage relationships (*I–V*) of PFC pyramidal cells. (*A*) Examples of *I–V* curves from inward rectifying neurons (left) and from non-rectifying neurons (right). Each point is the average of 10 values. The electrophysiological class of the cells is indicated by the symbols. (*B*) The responses to hyperpolarizing pulses (from –0.2 to –1.2 nA) of one cell in each different electrophysiological class are illustrated. The symbols in brackets refer to the corresponding curves in (*A*). Note the depolarizing sag for group I slow-adapting RS cell (filled arrow) and the depolarizing membrane potential at the break of the pulses for group I slow-adapting RS, NIB and IB cells (open arrows). Each trace is the average of 10 values.

superficial layers (Fig. 10) had a maximal basal dendritic extent of 120 μm dorso-ventrally and 150 μm rostro-caudally. The extent of its apical tuft in layer I was 350 μm dorso-ventrally and 250 μm rostro-caudally.

*IB Cells*

The three labeled IB cells had their soma located in layer V and presented a peculiar morphological feature (Figs 9*D* and 10). Their somas (370 ± 78 $\mu m^2$ area) were larger than those of deep layers NIB cells ($P < 0.05$). Their dendrites and spines appeared thicker than those of the cells from the two previous classes.

The maximal extent of the basal dendritic field of IB cells was significantly larger than that of deep layers RS and NIB cells, both along the dorso-ventral (337 ± 54 μm, $P < 0.05$, $P < 0.1$, respectively) and the rostro-caudal axes (330 ± 29 μm; $P < 0.05$, $P < 0.005$, respectively). The apical dendrite gave off branches within layer V, but only a few in layers II/III. As compared to deep layers RS and NIB cells, the apical tufts of IB cells were larger dorso-ventrally (500 ± 130 μm, $P < 0.005$, $P < 0.1$, respectively) and rostro-caudally (380 ± 104 μm, $P < 0.005$, $P < 0.05$, respectively).

**Table 2**
Repartition of soma of the pyramidal cells injected with neurobiotin in the different layers of the prefrontal cortex

| Electrophysiological classes | n | Layers II–III | Layer V | Layer VI |
|---|---|---|---|---|
| Slow-adapting RS | | | | |
| Group I | 18 | 1 | 11 | 6 |
| Group II | 9 | 2 | 4 | 3 |
| Fast-adapting RS | 3 | 2 | 1 | – |
| IB | 3 | – | 3 | – |
| NIB | 8 | 1 | 6 | 1 |

## Discussion

The present study aimed to characterize the *in vivo* electrophysiological properties of morphologically identified pyramidal cells in the rat PFC. Three main electrophysiological classes

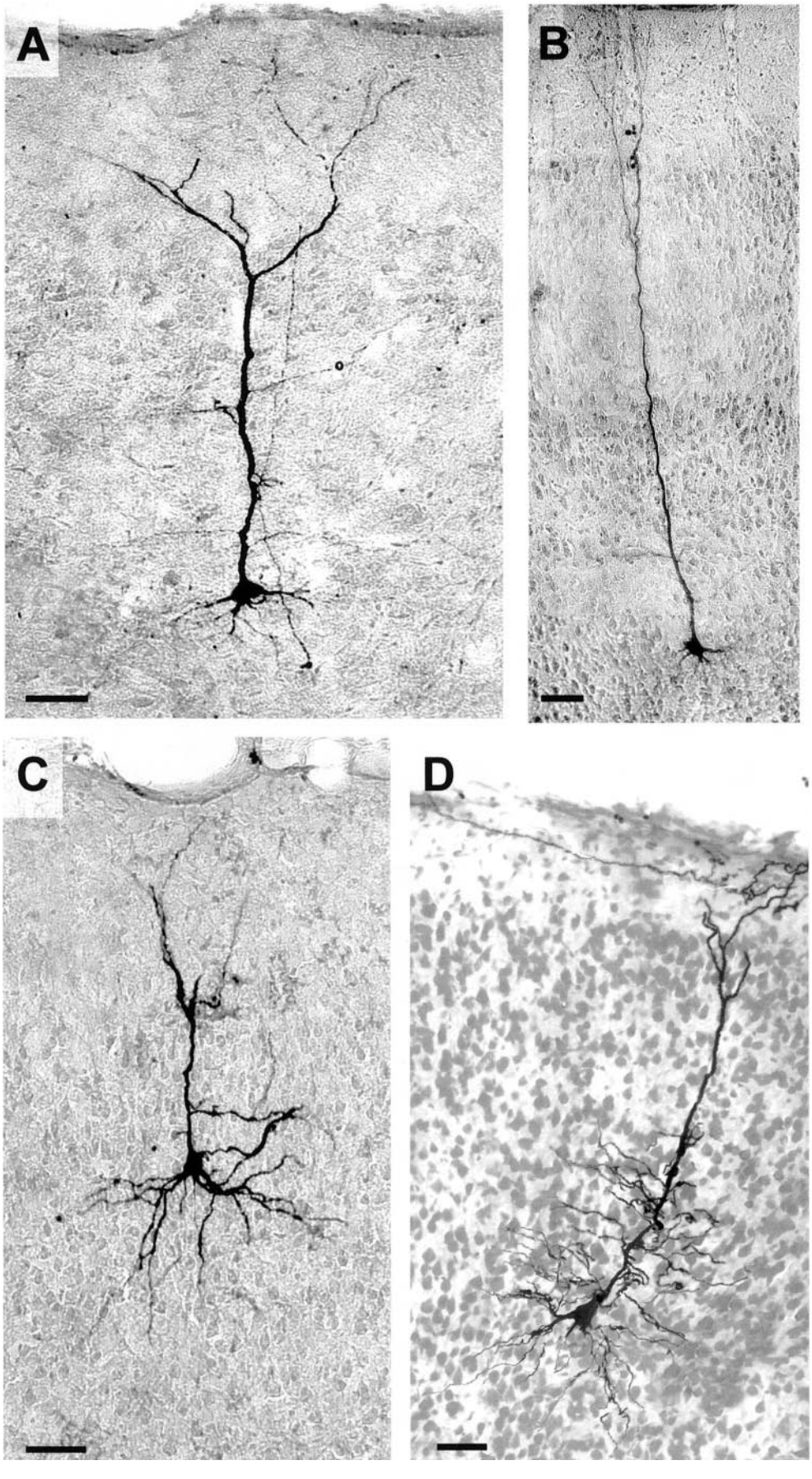
A
B
C
D

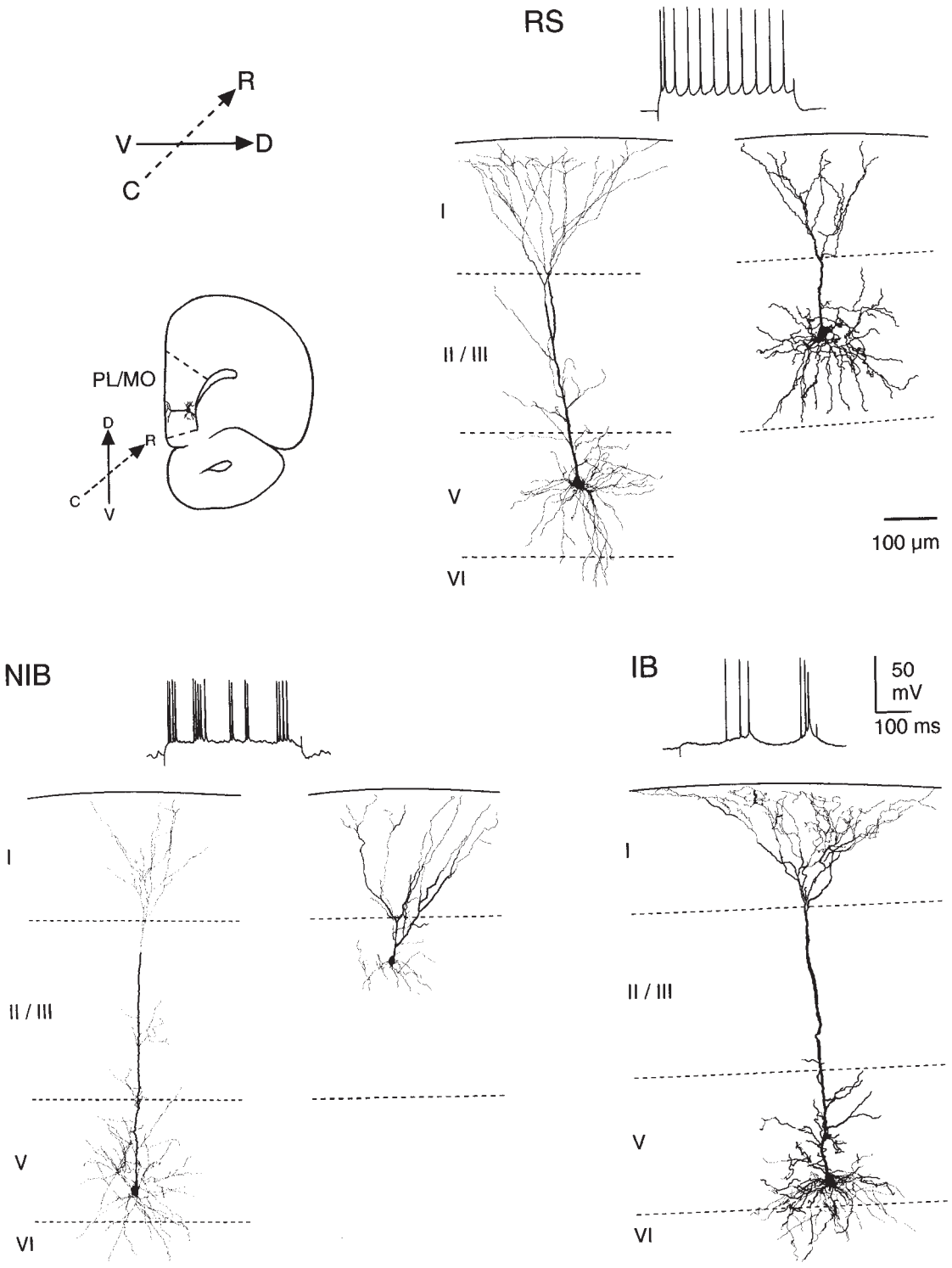


**Figure 10.** Neurolucida reconstructions of representative neurons from the three main electrophysiological classes of prefrontal pyramidal cells. Top, left: schematic representation of the orientation of a pyramidal cell within the prelimbic/medial orbital area in a frontal section. The arrows indicate the caudo-rostral (C-R) and the ventro-dorsal (V-D) axes of the brain section and of the reconstructed cells (upper left). Upper right panel: two slow-adapting RS cells (group I) with soma in deep and superficial layers, respectively. Bottom left panel: two NIB cells with soma in deep and superficial layers, respectively. Bottom right panel: an IB cell with soma in layer V. Note that NIB cells have a smaller soma and less developed dendritic fields than RS and IB cells and that the IB cell presents thick dendrites and a large dendritic extent. Insets: characteristic firing patterns of RS, NIB and IB cells.

**Figure 9.** Photomicrographs of neurobiotin-labeled pyramidal cells from different electrophysiological classes. (*A*) A slow-adapting RS cell (group I) with soma located in upper layer V. (*B*) An NIB cell with soma located in layer VI. (*C*) A slow-adapting RS cell (group I) which soma was located in layer III. (*D*) An IB cell with soma located in layer V; the electrophysiological properties of this cell are shown in Figure 6. Scale bars: 50 µm.

of pyramidal cells were distinguished on the basis of: (i) their firing pattern in response to depolarizing current pulses; (ii) the properties of their action potentials; and (iii) their spontaneous firing. In addition to the RS and IB cells previously described in PFC slices (de la Peña and Geijo-Barrientos, 1996; Yang *et al.*, 1996), we identified an additional class of pyramidal cells – the NIB cells – not yet described in cortical slices. Furthermore, the RS class is not homogenous and has been subdivided in slow-adapting and fast-adapting RS cells. Finally, the present *in vivo* data show that successive applications of identical depolarizing current pulses induced different patterns of discharge in NIB cells and in some RS cells, suggesting that synaptic input can participate in determining the discharge pattern of PFC cells.

### *Electrophysiological Characteristics of PFC Pyramidal Cells*

The classification of the different electrophysiological types of PFC pyramidal cells proposed in the present study has taken into account the previously reported classifications of cortical pyramidal cells. Because different terminologies have been used, we tentatively propose in Table 3 a correspondence between these terminologies and the classification proposed in the present study.

**Table 3**
Tentative correspondence between the electrophysiological classes described in the present (first column) and previous studies (third column) (the experimental conditions are indicated in the second column)

| | | | |
|---|---|---|---|
| RS | RS | slice, sensori-motor, guinea-pig | (Connors *et al.*, 1982) |
| | Group A | in vivo, motor, rat | (Pockberger, 1991) |
| | IB | slice, prefrontal, rat | (Yang *et al.*, 1996) |
| | Slow-adapting group I | | |
| | RS1 | slice, sensory, mouse | (Agmon and Connors, 1992) |
| | Intermediate | slice, sensori-motor, rat | (Van Brederode and Snyder, 1992) |
| | RS slow-adapting | in vivo, areas 5–7, cat | (Nuñez *et al.*, 1993) |
| | RS | slice, motor, rat | (Tseng and Prince, 1993) |
| | Slow-adapting group II | | |
| | RS | slice, sensori-motor and cingulate, guinea pig | (McCormick *et al.*, 1985) |
| | RS2 | slice, sensory, mouse | (Agmon and Connors, 1992) |
| | Phasic–tonic | slice, sensori-motor, rat | (Van Brederode and Snyder, 1992) |
| | Adapting | slice, motor, rat | (Tseng and Prince, 1993) |
| | RS | slice, prefrontal, rat | (Yang *et al.*, 1996) |
| | Fast-adapting | | |
| | RS fast-adapting | in vivo, areas 5–7, cat | (Nuñez *et al.*, 1993) |
| IB | IB (intrinsic-bursting) | slice, sensori-motor, guinea pig | (Connors *et al.*, 1982) |
| | Group B | in vivo, motor, rat | (Pockberger, 1991) |
| | IB (inactivating-bursting) | in vivo, motor, cat | (Baranyi *et al.*, 1993a) |
| | $RS_{DAP}$ | slice, motor, rat | (Tseng and Prince, 1993) |
| | ROB (repetitive-oscillatory-bursting) | slice, sensori-motor, rat<br>slice, prefrontal, rat | (Silva *et al.*, 1991)<br>(Yang *et al.*, 1996) |
| NIB | NIB (non-inactivating-bursting) | in vivo, motor, cat | (Baranyi *et al.*, 1993a) |

#### *RS Cells*

In agreement with previous *in vivo* (Nuñez *et al.*, 1993; Baranyi *et al.*, 1993a) and *in vitro* (Connors and Gutnick, 1990) recordings performed in several cortical areas, the present data indicate that RS cells constitute the main electrophysiological class of pyramidal neurons in the rat PFC. However, the RS class was not homogeneous (see Table 3) and was thus subdivided in slow- and fast-adapting RS cells.

Fast-adapting RS cells, which were characterized by an initial train of spikes in response to high intensity depolarizing current pulses, have been previously described in the cat association cortex *in vivo* (Nuñez *et al.*, 1993), but not in cortical slices. The initial evoked discharge was often followed by a slow membrane depolarization that might be due either to the activation of a specific conductance or to a synaptic response resulting from the activation of a local circuit. In the PFC, these cells were also characterized by a lack of spontaneous firing and, as in the association cortex, they represented a small proportion of RS cells.

Slow-adapting RS cells were further subdivided in two groups, according to previous *in vitro* studies (Agmon and Connors, 1992; Van Brederode and Snyder, 1992; Tseng and Prince, 1993). These two groups have been denominated groups I and II in the present study and likely correspond respectively to the IB and RS cells described in PFC slices by Yang *et al.* (Yang *et al.*, 1996) – see Table 3. In response to a prolonged depolarizing current pulse, group I cells presented an initial doublet or triplet of spikes followed by a sustained discharge with no obvious frequency adaptation, whereas group II cells showed an adaptation of their discharge frequency.

These two groups of RS neurons exhibited distinct intrinsic properties that could account for their distinct firing patterns. First, in response to application of positive current pulses, an initial doublet or triplet of action potentials was observed in all group I cells, but only 35% of group II cells. Such an initial high-frequency firing has also been described in pyramidal neurons from other cortical areas (McCormick *et al.*, 1985; Mason and Larkman, 1990; Agmon and Connors, 1992; Van Brederode and Snyder, 1992; Nuñez *et al.*, 1993; Baranyi *et al.*, 1993a; Kang and Kayano, 1994). In group I, but not in group II cells, the first action potential of the evoked firing was followed by a DAP. Interestingly, in the cat motor cortex, it has been reported that pyramidal cells with DAPs displayed no adaptation, while those lacking DAPs exhibited adaptation (Kang and Kayano, 1994).

Second, in response to hyperpolarizing current pulses, only the group I cells exhibited an initial depolarizing 'sag' and a depolarizing rebound at the cessation of the pulses. The initial 'sag' is classically attributed to the Ih current (Spain *et al.*, 1987). It has been proposed that the depolarizing rebound, also observed in RS cells of guinea pig parietal and medial frontal cortex slices (Friedman and Gutnick, 1987; de la Peña and Geijo-Barrientos, 1996), was due to a low threshold calcium current.

Third, during the sustained evoked discharge, the sAHPs of group I and group II cells presented distinct characteristics. Indeed, the sAHPs of group I cells were monophasic and those of group II cells were biphasic with a progressive lengthening of the second component that was correlated with an increase in the ISIs during spike frequency adaptation. In addition, the firing threshold remained constant in group I cells and progressively increased in group II cells. Thus, both the prolonged membrane hyperpolarization due to the second phase of the sAHP and the progressive increase in the firing threshold are likely to participate in spike frequency adaptation of group II cells. Recently, a negative correlation between spike threshold and the rate of membrane depolarization preceding the spike has been observed in cortical RS cells by Azouz and Gray (Azouz and Gray, 2000), who proposed that increases in spike threshold result from a decrease in the availability of $Na^+$ channels during slow depolarizations. It can be suggested that a similar process is involved in the progressive increase in firing threshold observed in group II RS cells in the present study.

*IB Cells*

As previously reported in other cortical areas (McCormick *et al*., 1985; Montoro *et al*., 1988; Chagnac-Amitai *et al*., 1990; Baranyi *et al*., 1993a; Tseng and Prince, 1993; Wang and McCormick, 1993), the ability to generate bursts in PFC IB cells was related to the level of membrane depolarization. Indeed, bursts of action potentials were mainly elicited with near-threshold depolarizing currents, while high-intensity currents induced repetitive firing similar to that of RS cells. In addition, at the cessation of a hyperpolarizing current pulse, bursts were also triggered in PFC IB cells. It can be suggested that a conductance partially inactivated at resting membrane potential, such as the low threshold calcium conductance, is likely involved in the generation of bursts (Carbone and Lux, 1984; Friedman and Gutnick, 1987; Sayer *et al*., 1990). On the other hand, as previously reported, single action potentials were followed by a DAP (Connors *et al*., 1982; Chagnac-Amitai *et al*., 1990; Baranyi *et al*., 1993b; Tseng and Prince, 1993; Yang *et al*., 1996). Finally, in the present study, IB cells were also characterized by a higher spontaneous firing frequency as compared with the other classes of pyramidal cells and by the occurrence of spontaneous bursts.

A small proportion (10–20%) of pyramidal neurons have been characterized as IB cells in different cortical areas either in anesthetized animals (Pockberger, 1991; Baranyi *et al*., 1993a; Nuñez *et al*., 1993) or in cortical slices (Connors *et al*., 1982; McCormick *et al*., 1985; Agmon and Connors, 1992). However, the proportion of pyramidal neurons displaying IB firing patterns may vary with experimental conditions. Indeed, as recently shown in cortical slabs, the percentage of IB cells is double that reported in intact cortex under anesthesia (Timofeev *et al*., 2000). In the present study, IB cells, found only in layer V, represented 7% of the total population of pyramidal neurons recorded in layers II–VI of the PFC. In PFC slices, the cells denominated 'repetitive oscillatory bursting' (ROB) by Yang *et al*. (Yang *et al*., 1996), which likely correspond to IB cells, represent a small proportion of pyramidal neurons recorded in layers V–VI.

*NIB Cells*

In contrast to IB cells, the bursts of which presented spike inactivation and were only evoked by near-threshold depolarizing currents, in NIB cells the spike amplitude was constant within the bursts and the probability of evoking bursts increased with membrane depolarization. However, as with IB cells, NIB cells discharged bursts spontaneously and had a higher spontaneous firing than the other classes of pyramidal cells. This class of cells has not been described *in vitro*, but has also been characterized in the motor cortex of the conscious cat (Baranyi *et al*., 1993a), where it represented, as in the present study, a significant proportion of pyramidal cells (22%). Since spontaneous synaptic activity is much lower *in vitro* than *in vivo*, it can be suggested that NIB cells have not been distinguished from RS cells *in vitro* because de-inactivation of some membrane conductances by a sustained synaptic activity might be required to elicit non-inactivating bursts.

*Subthreshold Membrane Potential Oscillations*

Under different anesthesia such as α-chloralose–, urethane– or ketamine–xylazine, the membrane potential of cortical neurons presented step-like membrane potential shifts called 'up' and 'down' states (Cowan and Wilson, 1994; Stern *et al*., 1997; Paré *et al*., 1998; Lewis and O'Donnell, 2000; Mahon *et al*., 2001). Such 'up' and 'down' states of membrane potential were not observed in the present study performed under pentobarbital anesthesia, suggesting that these oscillations depend on the type of anesthetic used. Indeed, a recent study shows that, in rat cortical neurons, low-frequency oscillations of the membrane potential occur under ketamine–xylazine, but not under barbiturate anesthesia (Mahon *et al*., 2001).

In cortical slices, high-frequency (10–50 Hz) membrane oscillations were detected in neurons upon subthreshold membrane depolarization (Llinas *et al*., 1991; Yang *et al*., 1996; Dickson *et al*., 2000). This phenomenon was not observed in previous *in vivo* studies, nor in the present work. It can be suggested that, *in vivo*, the intense spontaneous synaptic activity does not allow the observation of the fast membrane oscillations recorded in the cortical slices, in which the spontaneous synaptic events are rare.

### *Cell Morphology*

All the cells labeled after electrophysiological characterization were pyramidal neurons located in the prelimbic/medial orbital areas of the PFC. Their basal dendrites were mainly located within the same layer as the soma and their apical dendrites reached layer I, where they divided to form apical tufts. In the PFC, as previously reported in other cortical areas, the soma of RS cells was located from layer II to layer VI and that of IB cells in layer V (Chagnac-Amitai *et al*., 1990; Mason and Larkman, 1990). Even though no significant morphological difference could be established between RS and NIB cells, the soma of NIB cells were slightly smaller than in RS cells and the apical dendritic tree of deep layer NIB cells appeared less developed than in deep layer RS cells. On the contrary, IB cells have distinctly different morphological features from RS cells. As previously observed in slices of other cortical areas, the soma of IB cells in the PFC appeared larger and the apical dendrite thicker (Chagnac-Amitai *et al*., 1990; Mason and Larkman, 1990). In addition, the present *in vivo* study further confirms that the extent of the basal and the apical dendritic fields of IB cells was more widespread than that of RS cells. Finally, the soma and the extent of the dendritic field of IB cells were larger than in NIB cells. Thus, it could be suggested, on the basis of their morphological characteristics, that IB cells receive and integrate more numerous and complex inputs than RS and NIB cells.

The firing pattern of neurons is usually attributed to the types and densities of their ionic channels, but may also be influenced by their morphological features. Using compartmental models of reconstructed cortical neurons, Mainen and Sejnovski (Mainen and Sejnowski, 1996) have shown that various firing patterns can be reproduced in a set of neurons with a common distribution of ionic channels but with different dendritic geometry. This model predicts that sustained adapting and non-adapting discharge occurs for neurons with the smallest or moderate dendritic area, respectively, and that bursting is associated with the largest dendritic area. In agreement with this model, in the present study, bursting was observed in IB cells, which showed a more developed dendritic tree than RS cells. However, bursting was also observed in NIB cells, in which the dendritic tree was slightly smaller than that of RS and significantly less developed than that of IB cells. Such a discrepancy with this model likely results from the differences in the type and/or distribution of ionic channels.

### *Variability of the Firing Patterns*

The present study shows that, within a given class, the firing pattern of a cell can display some variability and/or be transformed into that of another class. Indeed, in response to successive identical depolarizing current pulses, NIB cells

displayed either bursts or an RS-like discharge and some slow-adapting RS cells exhibited either a regular firing pattern or an irregular discharge with large membrane hyperpolarizations. A transformation of the discharge pattern evoked by successive identical depolarizing current pulses has also been reported in fast-rhythmic-bursting neurons of the cat neocortex that changed their firing mode from rhythmic bursting to fast tonic spiking during barbiturate spindles (Steriade *et al*., 1998). Such variations in firing mode may result from fluctuations in the background synaptic activity, since they have not been described in cortical slices, in which spontaneous synaptic activity is rare. Recently, Paré *et al*. (Paré *et al*., 1998) have estimated the impact of spontaneous synaptic activity on the input resistance of neocortical pyramidal neurons. They have shown that in intact networks *in vivo* during high background synaptic activity the input resistance of the cells was much lower than in cortical slices. Accordingly, the input resistance of pyramidal neurons in the present study was much lower than that observed in the PFC slices (Yang *et al*., 1996). It can thus be suggested that the variability of the evoked discharge patterns observed in some PFC pyramidal neurons in anesthetized rats could result from variations of their input resistance due to fluctuations in synaptic activity.

Finally, in the present study, it was observed that by increasing the intensity of the depolarizing current pulses, the bursting features of IB cells changed into an RS-like firing pattern. Such a transformation of the discharge pattern of IB cells from bursting to regular spiking mode has been previously observed during arousal elicited by stimulating brainstem reticular formation (Steriade *et al*., 1993) as well as during natural transition from slow-wave sleep to REM sleep or waking (Steriade *et al*., 2001). Furthermore, in cortical slices, it has been shown that the slow membrane depolarization induced by activation of α1-adrenergic, muscarinic or metabotropic glutamate receptors results in a shift in the firing pattern of IB cells from bursting to RS mode of discharge (Wang and McCormick, 1993). These studies indicate that the firing mode of IB cells can be modulated by the action of several neurotransmitters.

Taken together, the present *in vivo* data allowed us to characterize distinct electrophysiological classes of pyramidal cells in the rat PFC. However, the firing pattern of these cells does not have invariant features, but results from an interaction between their intrinsic membrane properties and the nature of their synaptic inputs.

### *Functional Considerations*

The PFC plays a key role in high cognitive functions such as working memory and planning of actions. Electrophysiological studies in monkeys have shown that some PFC neurons display a sustained enhancement of firing during the delay period of delayed-response tasks that likely represents a cellular correlate of working memory (Suzuki and Azuma, 1977; Sakai and Hamada, 1981; Funahashi *et al*., 1989; Goldman-Rakic, 1995a,b; Miller *et al*., 1996; Fuster, 2001). In rat, an increased discharge of PFC neurons during delay has also been described in the prelimbic area (Orlov *et al*., 1988; Batuev *et al*., 1990). It is generally assumed that the sustained firing increase of PFC neurons during the delay period represents the active holding of the sensory stimuli and participates in the neural process ensuring correct performance of the task (Fuster, 1995; Goldman-Rakic, 1995a). The nature of the neuronal mechanisms underlying this sustained increase in the discharge is still poorly understood. It has been proposed that reentrant excitatory feedback cortical (posterior parietal cortex) and subcortical (mediodorsal nucleus of the thalamus) circuits cooperate to maintain an increased discharge in PFC neurons. In addition to these direct feedback circuits, the participation of the multisynaptic loop circuit involving the basal ganglia might also be suggested (Maurice *et al*., 1999). In addition to the involvement of these excitatory feedback networks, the ability of PFC neurons to maintain sustained discharge during the delay period is likely subordinated to the basic electrophysiological properties of the cells. Indeed, intrinsic membrane properties of neurons are critically involved in the integration of synaptic inputs into spike train output (Llinas, 1986; Schwindt, 1992). Among the different classes of cells described in the present study, it can be proposed that slow-adapting RS cells, in contrast to fast-adapting RS cells, present appropriate electrophysiological properties to maintain a sustained increase of firing during the delay period. Under certain conditions, IB cells can also present the properties required to maintain a sustained increase in firing. Indeed, IB cells transform their firing mode from bursting to RS-like by slightly increasing the direct depolarization as shown in the present study, or following activation of either α1-adrenergic, muscarinic or glutamate metabotropic receptors (Wang and McCormick, 1993; Steriade *et al*., 1993) or, finally, during natural waking as compared to slow-wave sleep (Steriade *et al*., 2001).

Dopamine transmission in the PFC plays an important role in modulating the processes in which short-term memory is used to guide goal-directed behavior. Indeed, prefrontal dopamine depletion or blockade of dopamine receptors in the PFC, in both monkeys and rats, causes severe deficits in delay tasks performance (Brozoski *et al*., 1979; Bubser and Schmidt, 1990; Sawagushi *et al*., 1990; Sawagushi and Goldman-Rakic, 1994; Zahrt *et al*., 1997). In monkeys performing working memory tasks, local application of a D1 dopamine receptors antagonist can selectively increase the activity of 'memory cells', while application of a D2 antagonist produces a non-selective reduction in neuronal activity (Williams and Goldman-Rakic, 1995). Recently, Durstewitz *et al*. (Durstewitz *et al*., 2000) have constructed a PFC network model predicting that one function of dopamine may be to stabilize the delay firing discharge and to protect it against interfering stimuli. Since, in peculiar conditions, dopamine can selectively modulate the activity of a given population of PFC neurons, it would be of interest to determine whether dopamine exerts distinct effects on the electrophysiological properties and synaptic inputs of the different classes of PFC pyramidal neurons characterized in the present work.

## Conclusions

We have identified *in vivo* three main electrophysiological classes of pyramidal cells in the rat prefrontal cortex on the basis of their specific discharge patterns in response to depolarizing current pulses. Although the firing patterns of the neurons basically depend on their intrinsic membrane properties, our data suggest that the ongoing spontaneous synaptic activity also participates in shaping the neuronal output activity. The strong synaptic activity occurring *in vivo* could explain why additional classes of cells were found in the present study as compared with those performed *in vitro*. Because the dynamic properties of cortical pyramidal neurons are critical for input–output information processing, knowledge of the intrinsic properties of the different classes of PFC pyramidal neurons, as well as of the influence exerted by their related neuronal network, is of importance for a more detailed understanding of the processes involved in the functions of the PFC, such as working memory (Compte *et al*., 2000).

## Notes

The authors would like to thank Dr S. Charpier for helpful scientific discussion. We thank S. Slaghth for critical reading of the manuscript, and A.M. Godeheu and M. Saffroy for histological assistance. E. Dégenètais is recipient of a fellowship from the Ministère de l'Enseignement Supérieur et de la Recherche. This work was supported by l'Institut National de la Santé et de la Recherche Médicale (INSERM).

Address correspondence to Yves Gioanni, INSERM U114, Chaire de Neuropharmacologie, Collège de France, 11, place Marcelin Berthelot, 75231 Paris Cedex 05, France. Email: yves.gioanni@college-de-france.fr.

## References

Agmon A, Connors BW (1992) Correlation between intrinsic firing patterns and thalamocortical synaptic responses of neurons in mouse barrel cortex. J Neurosci 12:319–329.

Azouz R, Gray M (2000) Dynamic spike threshold reveals a mechanism for synaptic coincidence detection in cortical neurons *in vivo*. Proc Natl Acad Sci USA 97:8110–8115.

Baranyi A, Szente MB, Woody CD (1993a) Electrophysiological characterization of different types of neurons recorded *in vivo* in the motor cortex of the cat. I. Patterns of firing activity and synaptic responses. J Neurophysiol 69:1850–1864.

Baranyi A, Szente MB, Woody CD (1993b) Electrophysiological characterization of different types of neurons recorded *in vivo* in the motor cortex of the cat. II. Membrane parameters, action potentials, current-induced voltage responses and electrotonic structures. J Neurophysiol 69:1865–1879.

Batuev A, Kursina NP, Shutov AP (1990) Unit activity of the medial wall of the frontal cortex during delayed performance in rats. Behav Brain Res 41:95–102.

Brozowski TS, Brown RM, Rosvold HE, Goldman PS (1979) Cognitive deficits caused by regional depletion of dopamine in prefrontal cortex of Rhesus monkey. Science 205:929–932.

Bubser M, Schmidt WJ (1990) 6-Hydroxydopamine lesion of the rat prefrontal cortex increases locomotor activity, impairs acquisition of delayed alternation tasks, but does not affect uninterrupted tasks in the radial maze. Behav Brain Res 37:157–168.

Carbone E, Lux HD (1984) A low voltage-activated, fully inactivating Ca channel in vertebrate sensory neurons. Nature 310:501–502.

Chagnac-Amitai Y, Luhmann HJ, Prince DA (1990) Burst generating and regular spiking layer 5 pyramidal neurons of rat neocortex have different morphological features. J Comp Neurol 296:598–613.

Compte A, Brunel N, Goldman-Rakic PS, Wang X-I (2000) Synaptic mechanisms and network dynamics underlying spatial working memory in a cortical network model. Cereb Cortex 10:910–923.

Connors BW, Gutnick MJ (1990) Intrinsic firing pattern of diverse neocortical neurons. Trends Neurosci 13:99–104.

Connors BW, Gutnick MJ, Prince DA (1982) Electrophysiological properties of neocortical neurons *in vitro*. J Neurophysiol 48: 1302–1320.

Cowan RL, Wilson CJ (1994) Spontaneous firing patterns and axonal projections of single corticostriatal neurons in the rat medial agranular cortex. J Neurophysiol 71:17–32.

de la Peña E, Geijo-Barrientos E (1996) Laminar localization, morphology and physiological properties of pyramidal neurons that have the low-threshold calcium current in the guinea-pig medial frontal cortex. J Neurosci 16:5301–5311.

Dickson CT, Magistretti J, Shalinsky M, Hamam B, Alonso A (2000) Oscillatory activity in entorhinal neurons and circuits. Ann NY Acad Sci 911:127–150.

Durstewitz D, Seamans JK, Sejnowski TJ (2000) Dopamine-mediated stabilization of delay-period activity in a network model of prefrontal cortex. J Neurophysiol 83:1733–1750.

Floresco SB, Seamans JK, Phillips AG (1997) Selective roles for hippocampal, prefrontal cortical and ventral striatal circuits in radial-arm maze tasks with or without a delay. J Neurosci 17:1880–1890.

Friedman A, Gutnick M (1987) Low-threshold calcium electrogenesis in neocortical neurons. Neurosci Lett 81:117–122.

Funahashi S, Bruce CJ, Goldman-Rakic PS (1989) Mnemonic coding of visual space in the monkey's dorsolateral prefrontal cortex. J Neurophysiol 61:331–349.

Fuster JM (1995) Memory in the cerebral cortex: an empirical approach to neural networks in the human and nonhuman primate. Cambridge, MA: MIT.

Fuster JM (1997) The prefrontal cortex: anatomy, physiology and neuropsychology of the frontal lobe. Philadelphia, PA: Lippincott-Raven.

Fuster JM (2001) The prefrontal cortex — an update: time is of the essence. Neuron 30:319–333.

Goldman-Rakic PS (1995a) Cellular basis of working memory. Neuron 14: 477–485.

Goldman-Rakic PS (1995b) Toward a circuit model of working memory and the guidance of voluntary motor action. In: Models of information processing in the basal ganglia (Houk JC, Dacis JC, Beiser DG, eds), ch. 7, pp. 131–148. Cambridge, MA: Bradford Book, MIT.

Groenewegen HJ (1988) Organization of afferent connections of mediodorsal thalamic nucleus in the rat, related to mediodorsal–prefrontal topography. Neuroscience 24:397–431.

Kang Y, Kayano F (1994) Electrophysiological and morphological characteristics of layer VI pyramidal cells in the cat motor cortex. J Neurophysiol 72:578–592.

Lewis BL, O'Donnell P (2000) Ventral tegmental area afferents to the prefrontal cortex maintain membrane potential 'up' states in pyramidal neurons via D1 dopamine receptors. Cereb Cortex 10: 1168–1175.

Llinas RR (1986) Intrinsic electrophysiological properties of mammalian neurons: insights into the central nervous system functions. Science 242:1654–1664.

Llinas RR, Grace AA, Yarom Y (1991) *In vitro* neurons in mammalian cortical layer 4 exhibit intrinsic oscillatory activity in the 10- to 50-Hz frequency range. Proc Natl Acad Sci USA 88:897–901.

Mahon S, Deniau JM, Charpier S (2001) Relationship between EEG potentials and intracellular activity of striatal and cortico-striatal neurons: an *in vivo* study under different anesthetics. Cereb Cortex 11:360–373.

Mainen ZF, Sejnowski TJ (1996) Influence of dendritic structure on firing pattern in model neocortical neurons. Nature 382:363–366.

Mason A, Larkman A (1990) Correlation between morphology and electrophysiology of pyramidal neurons in slices of rat visual cortex. II. Electrophysiology. J Neurosci 10:1415–1428.

Maurice N, Deniau JM, Glowinski J, Thierry AM (1999) Relationships between the prefrontal cortex and the basal ganglia in the rat: physiology of the cortico-nigral circuits. J Neurosci 19:4674–4681.

McCormick DA, Connors BW, Lighthall JW, Prince DA (1985) Comparative electrophysiology of pyramidal and sparsely spiny stellate neurons of the neocortex. J Neurophysiol 54:782–806.

Miller EK, Erickson CA, Desimone R (1996) Neural mechanisms of visual working memory in prefrontal cortex of the macaque. J Neurosci 16:5154–5167.

Montoro RJ, Lopez-Barneo J, Jassik-Gerschenfeld D (1988) Differential burst firing modes in neurons of the mammalian visual cortex *in vitro*. Brain Res 460:168–172.

Nuñez A, Amzica F, Steriade M (1993) Electrophysiology of cat association cortical cells *in vivo*: intrinsic properties and synaptic responses. J Neurophysiol 70:418–430.

Orlov AA, Kurzina NP, Shutov AP (1988) Activity of medial wall neurons in frontal cortex of rat brain during delayed response reactions. Neurosci Behav Physiol 18:31–37.

Paré D, Shink E, Gaudreau H, Destexhe A, Lang EJ (1998) Impact of spontaneous synaptic activity on the resting properties of cat neocortical pyramidal neurons *in vivo*. J Neurophysiol 79:1450–1460.

Paxinos G, Watson, C (1997) The rat brain in stereotaxic coordinates, 3rd edn. San Diego, CA: Academic Press.

Pockberger H (1991) Electrophysiological and morphological properties of rat motor cortex neurons *in vivo*. Brain Res 539:181–190.

Rose JE, Woolsey CN (1948) The orbito-frontal cortex and its connections with the mediodorsal nucleus of the rabbit, sheep and cat. Res Publ Assoc Ner Ment Dis 27:210–232.

Sakai M, Hamada I (1981) Intracellular activity and morphology of the prefrontal neurons related to visual attention task in behaving monkeys. Exp Brain Res 41:195–198.

Sawagushi T, Goldman-Rakic PS (1994) The role of D1-dopamine receptor in working memory: local injections of dopamine antagonists into the prefrontal cortex of rhesus monkeys performing an oculomotor delayed-response task. J Neurophysiol 71:515–528.

Sawagushi T, Matsumura M, Kubota K (1990) Effects of dopamine antagonists on neuronal activity related to a delayed response task in monkey prefrontal cortex. J Neurophysiol 63:1401–1412.

Sayer RJ, Schwindt PC, Crill WE (1990) High- and low-threshold calcium

currents in neurons acutely isolated from rat sensorimotor cortex. Neurosci Lett 120:175–178.

Schwindt PC (1992) Ionic currents governing input–output relations of Betz cells. In: Single neuron computation (McKenna T, Davis J, Zornetzer SF, eds), pp. 235–258. New York: Academic Press.

Seamans JK, Floresco SB, Phillips AG (1995) Functional differences between the prelimbic and anterior cingulate regions of the rat prefrontal cortex. Behav Neurosci 109:1–11.

Silva LR, Amitai Y, Connors BW (1991) Intrinsic oscillations of neocortex generated by layer 5 pyramidal neurons. Science 251:432–435.

Spain WJ, Schwindt PC, Crill WE (1987) Anomalous rectification in neurons from cat sensorimotor cortex *in vitro*. J Neurophysiol 57:1555–1576.

Stafstrom CE, Schwindt PC, Crill WE (1984) Repetitive firing in layer V neurons from cat neocortex *in vitro*. J Neurophysiol 52:264–277.

Steriade M, Amzica F, Nuñez A (1993) Cholinergic and noradrenergic modulation of the slow (~0.3 Hz) oscillation in neocortical cells. J Neurophysiol 70:1384–1400.

Steriade M, Timofeev I, Dürmüller N, Grenier F (1998) Dynamic properties of corticothalamic neurons and local cortical interneurons generating fast rhythmic (30–40 Hz) spike bursts. J Neurophysiol 79:483–490.

Steriade M, Timofeev I, Grenier F (2001) Natural waking and sleep states: a view from inside cortical neurons. J Neurophysiol 85:1969–1985.

Stern EA, Kincaid AE, Wilson CJ (1997) Spontaneous subthreshold membrane potential fluctuations and action potential variability of rat corticostriatal and striatal neurons *in vivo*. J Neurophysiol 77:1697–1715.

Suzuki H, Azuma M (1977) Prefrontal neuronal activity during gazing at light spot in the monkey. Brain Res 126:497–508.

Timofeev I, Grenier F, Bazhenov M, Sejnowski TJ, Steriade M (2000) Origin of slow cortical oscillations in deafferented cortical slabs. Cereb Cortex 10:1185–1199.

Tseng G-F, Prince DA (1993) Heterogeneity of rat corticospinal neurons. J Comp Neurol 335:92–108.

Uylings HBM, Van Eden CG (1990) Qualitative and quantitative comparison of the prefrontal cortex in rat and primates, including humans. In: The prefrontal cortex: its structure, function and pathology (Uylings HBM, Van Eden GC, De Bruin JPC, Corner MA, Feenstra MGP, eds), pp 31–62.Amsterdam: Elsevier.

Van Brederode JFM, Snyder GL (1992) A comparison of the electrophysiological properties of morphologically identified cells in layers 5b and 6 of the rat neocortex. Neuroscience 50:315–337.

Wang Z, McCormick DA (1993) Control of firing mode of corticotectal and corticopontine layer V burst-generating neurons by norepinephrine, acetylcholine and 1S, 3R-ACPD. J Neurosci 13:2199–2216.

Williams GV, Goldman-Rakic PS (1995) Modulation of memory fields by dopamine D1 receptors in prefrontal cortex. Nature 376:572–575.

Yang CR, Seamans JK (1996) Dopamine D1 receptor actions in layers V–VI rat prefrontal cortex neurons *in vitro*: modulation of dendritic–somatic signal integration. J Neurosci 16:1922–1935.

Yang CR, Seamans JK, Gorelova N (1996) Electrophysiological and morphological properties of layers V–VI principal pyramidal cells in rat prefrontal cortex *in vitro*. J Neurosci 16:1904–1921.

Zahrt J, Taylor RJ, Arnsten AFT (1997) Supranormal stimulation of D1 dopamine receptors in the rodent prefrontal cortex impairs working memory performance. J Neurosci 17:8528–8535.